

# A linear-time algorithm for the geodesic center of a simple polygon

Hee-Kap Ahn<sup>\*3</sup>, Luis Barba<sup>1,2</sup>, Prosenjit Bose<sup>1</sup>, Jean-Lou de Carufel<sup>1</sup>, Matias Korman<sup>4,5</sup>, and Eunjin Oh<sup>3</sup>

<sup>1</sup> School of Computer Science, Carleton University, Ottawa, Canada.

jit@scs.carleton.ca, jdecaruf@cg.scs.carleton.ca

<sup>2</sup> Département d'Informatique, Université Libre de Bruxelles, Brussels, Belgium.

lbarbafl@ulb.ac.be

<sup>3</sup> Department of Computer Science and Engineering, POSTECH,

77 Cheongam-Ro, Nam-Gu, Pohang, Gyeongbuk, Korea.

heekap@postech.ac.kr

<sup>4</sup> National Institute of Informatics (NII), Tokyo, Japan.

korman@nii.ac.jp

<sup>5</sup> JST, ERATO, Kawarabayashi Large Graph Project.

## Abstract

Given two points in a simple polygon  $P$  of  $n$  vertices, its geodesic distance is the length of the shortest path that connects them among all paths that stay within  $P$ . The geodesic center of  $P$  is the unique point in  $P$  that minimizes the largest geodesic distance to all other points of  $P$ . In 1989, Pollack, Sharir and Rote [Disc. & Comput. Geom. 89] showed an  $O(n \log n)$ -time algorithm that computes the geodesic center of  $P$ . Since then, a longstanding question has been whether this running time can be improved (explicitly posed by Mitchell [Handbook of Computational Geometry, 2000]). In this paper we affirmatively answer this question and present a linear time algorithm to solve this problem.

## 1 Introduction

Let  $P$  be a simple polygon with  $n$  vertices. Given two points  $x, y$  in  $P$ , the *geodesic path*  $\pi(x, y)$  is the shortest-path contained in  $P$  connecting  $x$  with  $y$ . If the straight-line segment connecting  $x$  with  $y$  is contained in  $P$ , then  $\pi(x, y)$  is a straight-line segment. Otherwise,  $\pi(x, y)$  is a polygonal chain whose vertices (other than its endpoints) are reflex vertices of  $P$ . We refer the reader to [19] for more information on geodesic paths.

The *geodesic distance* between  $x$  and  $y$ , denoted by  $|\pi(x, y)|$ , is the sum of the Euclidean lengths of each segment in  $\pi(x, y)$ . Throughout this paper, when referring to the distance between two points in  $P$ , we refer to the geodesic distance between them. Given a point  $x \in P$ , a (geodesic) *farthest neighbor* of  $x$ , is a point  $f_P(x)$  (or simply  $f(x)$ ) of  $P$  whose geodesic distance to  $x$  is maximized. To ease the description, we assume that each vertex of  $P$  has a unique farthest neighbor. We can make this *general position* assumption using simulation of simplicity [9].

Let  $F_P(x)$  be the function that, for each  $x \in P$ , maps to the distance to a farthest neighbor of  $x$  (i.e.,  $F_P(x) = |\pi(x, f(x))|$ ). A point  $c_P \in P$  that minimizes  $F_P(x)$  is called the *geodesic center* of  $P$ . Similarly, a point  $s \in P$  that maximizes  $F_P(x)$  (together with its farthest neighbor) is called a *geodesic diametral pair* and their distance is known as

\* The work by H.-K. Ahn and E. Oh was supported by the NRF grant 2011-0030044 (SRC-GAIA) funded by the Korea government (MSIP).



licensed under Creative Commons License CC-BY



Leibniz International Proceedings in Informatics  
Schloss Dagstuhl – Leibniz-Zentrum für Informatik, Dagstuhl Publishing, Germany

the *geodesic diameter*. Asano and Toussaint [3] showed that the geodesic center is unique (whereas it is easy to see that several geodesic diametral pairs may exist).

In this paper, we show how to compute the geodesic center of  $P$  in  $O(n)$  time. Due to lack of space, some proofs are omitted. A full version of the paper with all the omitted proofs can be found in the Appendix.

## 1.1 Previous Work

Since the early 1980s the problem of computing the geodesic center (and its counterpart, the geodesic diameter) has received a lot of attention from the computational geometry community. Chazelle [7] gave the first algorithm for computing the geodesic diameter (which runs in  $O(n^2)$  time using linear space). Afterwards, Suri [24] reduced it to  $O(n \log n)$ -time without increasing the space constraints. Finally, Hershberger and Suri [13] presented a fast matrix search technique, one application of which is a linear-time algorithm for computing the diameter.

The first algorithm for computing the geodesic center was given by Asano and Toussaint [3], and runs in  $O(n^4 \log n)$ -time. In 1989, Pollack, Sharir, and Rote [22] improved it to  $O(n \log n)$  time. Since then, it has been an open problem whether the geodesic center can be computed in linear time (indeed, this problem was explicitly posed by Mitchell [19, Chapter 27]).

Several other variations of these two problems have been considered. Indeed, the same problem has been studied under different metrics. Namely, the  $L_1$  geodesic distance [6], the link distance [23, 14, 8] (where we look for the path with the minimum possible number of bends or *links*), or even rectilinear link distance [20, 21] (a variation of the link distance in which only isothetic segments are allowed). The diameter and center of a simple polygon for both the  $L_1$  and rectilinear link metrics can be computed in linear time (whereas  $O(n \log n)$  time is needed for the link distance).

Another natural extension is the computation of the diameter and center in polygonal domains (i.e., polygons with one or more holes). Polynomial time algorithms are known for both the diameter [4] and center [5], although the running times are significantly larger (i.e.,  $O(n^{7.73})$  and  $O(n^{12+\varepsilon})$ , respectively).

## 1.2 Outline

In order to compute the geodesic center, Pollack *et al.* [22] introduce a linear time *chord-oracle*. Given a chord  $C$  that splits  $P$  into two sub-polygons, the oracle determines which sub-polygon contains  $c_P$ . Combining this operation with an efficient search on a triangulation of  $P$ , Pollack *et al.* narrow the search of  $c_P$  within a triangle (and find the center using optimization techniques). Their approach however, does not allow them to reduce the complexity of the problem in each iteration, and hence it runs in  $\Theta(n \log n)$  time.

The general approach of our algorithm described in Section 6 is similar: partition  $P$  into  $O(1)$  cells, use an oracle to determine which cell contains  $c_P$ , and recurse within the cell. Our approach differs however in two important aspects that allows us to speed-up the algorithm. First, we do not use the chords of a triangulation of  $P$  to partition the problem into cells. We use instead a cutting of a suitable set of chords. Secondly, we compute a set  $\Phi$  of  $O(n)$  functions, each defined in a triangular domain contained in  $P$ , such that their upper envelope,  $\phi(x)$ , coincides with  $F_P(x)$ . Thus, we can “ignore” the polygon  $P$  and focus only on finding the minimum of the function  $\phi(x)$ .

The search itself uses  $\varepsilon$ -nets and cutting techniques, which certify that both the size of the cell containing  $c_P$  and the number of functions of  $\Phi$  defined in it decrease by a constant

fraction (and thus leads to an overall linear time algorithm). This search has however two stopping conditions, (1) reach a subproblem of constant size, or (2) find a convex trapezoid containing  $c_P$ . In the latter case, we show that  $\phi(x)$  is a convex function when restricted to this convex trapezoid. Thus, finding its minimum becomes an optimization problem that we solve in Section 7 using cuttings in  $\mathbb{R}^3$ .

The key of this approach lies in the computation of the functions of  $\Phi$  and their triangular domains. Each function  $g(x)$  of  $\Phi$  is defined in a triangular domain  $\Delta$  contained in  $P$  and is associated to a particular vertex  $w$  of  $P$ . Intuitively speaking,  $g(x)$  maps points in  $\Delta$  to their (geodesic) distance to  $w$ . We guarantee that, for each point  $x \in P$ , there is one function  $g$  defined in a triangle containing  $x$ , such that  $g(x) = F_P(x)$ . To compute these triangles and their corresponding functions, we proceed as follows.

In Section 3, we use the matrix search technique introduced by Hershberger and Suri [13] to decompose the boundary of  $P$ , denoted by  $\partial P$ , into connected edge disjoint chains. Each chain is defined by either (1) a consecutive list of vertices that have the same farthest neighbor  $v$  (we say that  $v$  is *marked* if it has such a chain associated to it), or (2) an edge whose endpoints have different farthest neighbors (such edge is called a *transition edge*).

In Section 4, we consider each transition edge  $ab$  of  $\partial P$  independently and compute its *hourglass*. Intuitively, the hourglass of  $ab$ ,  $H_{ab}$ , is the region of  $P$  between two chains, the edge  $ab$  and the chain of  $\partial P$  that contains the farthest neighbors of all points in  $ab$ . Inspired by a result of Suri [24], we show that the sum of the complexities of each hourglass defined on a transition edge is  $O(n)$ . In addition, we provide a new technique to compute each of these hourglasses in linear time.

In Section 5 we show how to compute the functions in  $\Phi$  and their respective triangles. We distinguish two cases: (1) Inside each hourglass  $H_{ab}$  of a transition edge, we use a technique introduced by Aronov et al. [2] that uses the shortest-path trees of  $a$  and  $b$  in  $H_{ab}$  to decompose  $H_{ab}$  into  $O(|H_{ab}|)$  triangles with their respective functions (for more information on shortest-path trees refer to [10]). (2) For each marked vertex  $v$  we compute triangles that encode the distance from  $v$ . Moreover, we guarantee that these triangles cover every point of  $P$  whose farthest neighbor is  $v$ . Overall, we compute the  $O(n)$  functions of  $\Phi$  in linear time.

## 2 Hourglasses and Funnels

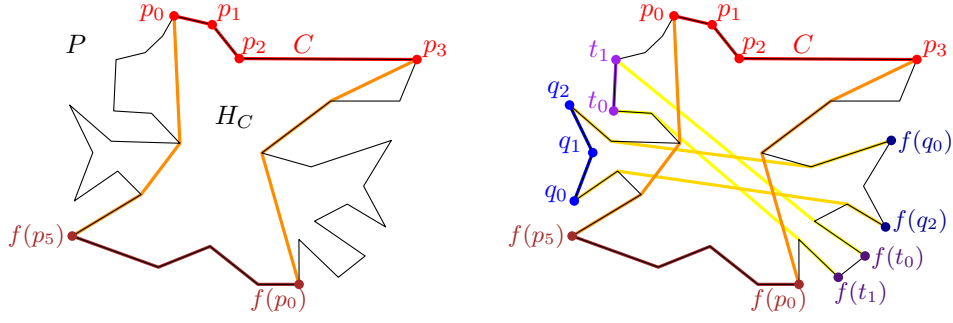
In this section, we introduce the main tools that are going to be used by the algorithm. Some of the results presented in this section have been shown before in different papers.

### 2.1 Hourglasses

Given two points  $x$  and  $y$  on  $\partial P$ , let  $\partial P(x, y)$  be the polygonal chain that starts at  $x$  and follows the boundary of  $P$  clockwise until reaching  $y$ .

For any polygonal chain  $C = \partial P(p_0, p_1, \dots, p_k)$ , the *hourglass* of  $C$ , denoted by  $H_C$ , is the simple polygon contained in  $P$  bounded by  $C$ ,  $\pi(p_k, f(p_0))$ ,  $\partial P(f(p_0), f(p_k))$  and  $\pi(f(p_k), p_0)$ ; see Figure 1. We call  $C$  and  $\partial P(f(p_0), f(p_k))$  the *top* and *bottom* chains of  $H_C$ , respectively, while  $\pi(p_k, f(p_0))$  and  $\pi(f(p_k), p_0)$  are referred to as the *walls* of  $H_C$ .

We say that the hourglass  $H_C$  is *open* if its walls are vertex disjoint. We say  $C$  is a *transition chain* if  $f(p_0) \neq f(p_k)$  and neither  $f(p_0)$  nor  $f(p_k)$  are interior vertices of  $C$ . In particular, if an edge  $ab$  of  $\partial P$  is a transition chain, we say that it is a *transition edge* (see Figure 1).



■ **Figure 1** Given two edge disjoint transition chains, their hourglasses are open and the bottom chains of their hourglasses are also edge disjoint. Moreover, these bottom chains appear in the same cyclic order as the top chains along  $\partial P$ .

130 ► **Lemma 1.** [Rephrase of Lemma 3.1.3 of [2]] If  $C$  is a transition chain of  $\partial P$ , then the  
131 hourglass  $H_C$  is an open hourglass.

132 Note that by Lemma 1, the hourglass of each transition chain is open. In the remainder  
133 of the paper, all the hourglasses considered are defined by a transition chain, i.e., they are  
134 open and their top and bottom chains are edge disjoint.

135 The following lemma is depicted in Figure 1 and is a direct consequence of the Ordering  
136 Lemma proved by Aronov et al. [2, Corollary 2.7.4].

137 ► **Lemma 2.** Let  $C_1, C_2, C_3$  be three edge disjoint transition chains of  $\partial P$  that appear in this  
138 order when traversing clockwise the boundary of  $P$ . Then, the bottom chains of  $H_{C_1}, H_{C_2}$  and  
139  $H_{C_3}$  are also edge disjoint and appear in this order when traversing clockwise the boundary  
140 of  $P$ .

141 Let  $\gamma$  be a geodesic path joining two points on the boundary of  $P$ . We say that  $\gamma$  *separates*  
142 two points  $x_1$  and  $x_2$  of  $\partial P$  if the points of  $X = \{x_1, x_2\}$  and the endpoints of  $\gamma$  alternate  
143 along the boundary of  $P$  ( $x_1$  and  $x_2$  could coincide with the endpoints of  $\gamma$  in degenerate  
144 cases). We say that a geodesic  $\gamma$  *separates* an hourglass  $H$  if it separates the points of its  
145 top chain from those of its bottom chain.

146 ► **Lemma 3.** Let  $C_1, \dots, C_r$  be edge disjoint transition chains of  $\partial P$ . Then, there is a set  
147 of  $t = O(1)$  geodesic paths  $\gamma_1, \dots, \gamma_t$  with endpoints on  $\partial P$  such that for each  $1 \leq i \leq r$  there  
148 exists  $1 \leq j \leq t$  such that  $\gamma_j$  separates  $H_{C_i}$ . Moreover, this set can be computed in  $O(n)$   
149 time.

150 A *chord* of  $P$  is an edge joining two non-adjacent vertices  $a$  and  $b$  of  $P$  such that  $ab \subseteq P$ .  
151 Therefore, a chord splits  $P$  into two sub-polygons.

152 ► **Lemma 4.** [Rephrase of Lemma 3.4.3 of [2]] Let  $C_1, \dots, C_r$  be a set of edge disjoint  
153 transition chains of  $\partial P$  that appear in this order when traversing clockwise the boundary of  
154  $P$ . Then each chord of  $P$  appears in  $O(1)$  hourglasses among  $H_{C_1}, \dots, H_{C_r}$ .

155 ► **Lemma 5.** Let  $x, u, y, v$  be four vertices of  $P$  that appear in this cyclic order in a clockwise  
156 traversal of  $\partial P$ . Given the shortest-path trees  $T_x$  and  $T_y$  of  $x$  and  $y$  in  $P$ , respectively, such  
157 that  $T_x$  and  $T_y$  can answer lowest common ancestor (LCA) queries in  $O(1)$  time, we can  
158 compute the path  $\pi(u, v)$  in  $O(|\pi(u, v)|)$  time. Moreover, all edges of  $\pi(u, v)$ , except perhaps  
159 one, belong to  $T_x \cup T_y$ .

► **Lemma 6.** *Let  $P$  be a simple polygon with  $n$  vertices. Given  $k$  disjoint transition chains  $C_1, \dots, C_k$  of  $\partial P$ , it holds that*

$$\sum_{i=1}^k |H_{C_i}| = O(n).$$

**Proof.** Because the given transition chains are disjoint, Lemma 2 implies that the bottom chains of their respective hourglasses are also disjoint. Therefore, the sum of the complexities of all the top and bottom chains of these hourglasses is  $O(n)$ . To bound the complexity of their walls we use Lemma 4. Since no chord is used more than a constant number of times, it suffices to show that the total number of chords used by all these hourglasses is  $O(n)$ .

To prove this, we use Lemma 3 to construct  $O(1)$  *split chains*  $\gamma_1, \dots, \gamma_t$  such that for each  $1 \leq i \leq k$ , there is a split chain  $\gamma_j$  that separates the top and bottom chains of  $H_{C_i}$ . For each  $1 \leq j \leq t$ , let

$$\mathcal{H}^j = \{H_{C_i} : \text{the top and bottom chain of } H_{C_i} \text{ are separated by } \gamma_j\}.$$

Since the complexity of the shortest-path trees of the endpoints of  $\gamma_j$  is  $O(n)$  [10], and from the fact that the chains  $C_1, \dots, C_k$  are disjoint, Lemma 5 implies that the total number of edges in all the hourglasses of  $\mathcal{H}^j$  is  $O(n)$ . Moreover, because each of these edges appears in  $O(1)$  hourglasses among  $C_1, \dots, C_k$ , we conclude that  $\sum_{H \in \mathcal{H}^j} |H| = O(n)$ . Since we have only  $O(1)$  split chains, our result follows. ◀

## 2.2 Funnels

Let  $C = (p_0, \dots, p_k)$  be a chain of  $\partial P$  and let  $v$  be a vertex of  $P$  not in  $C$ . The *funnel* of  $v$  to  $C$ , denoted by  $S_v(C)$ , is the simple polygon bounded by  $C$ ,  $\pi(p_k, v)$  and  $\pi(v, p_0)$ ; see Figure 2 (a). Note that the paths  $\pi(v, p_k)$  and  $\pi(v, p_0)$  may coincide for a while before splitting into disjoint chains. See Lee and Preparata [15] or Guibas et al. [10] for more details on funnels.

A subset  $R \subset P$  is *geodesically convex* if for every  $x, y \in R$ , the path  $\pi(x, y)$  is contained in  $R$ . This funnel  $S_v(C)$  is also known as the geodesic convex hull of  $C$  and  $v$ , i.e., the minimum geodesically convex set that contains  $v$  and  $C$ .

Given two points  $x, y \in P$ , the (geodesic) *bisector* of  $x$  and  $y$  is the set of points contained in  $P$  that are equidistant from  $x$  and  $y$ . This bisector is a curve, contained in  $P$ , that consists of circular arcs and hyperbolic arcs. Moreover, this curve intersects  $\partial P$  only at its endpoints [1, Lemma 3.22]. The (farthest) *Voronoi region* of a vertex  $v$  of  $P$  is the set of points  $R(v) = \{x \in P : F_P(x) = |\pi(x, v)|\}$  (including boundary points).

► **Lemma 7.** *Let  $v$  be a vertex of  $P$  and let  $C$  be a transition chain such  $R(v) \cap \partial P \subseteq C$  and  $v \notin C$ . Then,  $R(v)$  is contained in the funnel  $S_v(C)$*

## 3 Decomposing the boundary

In this section, we decompose the boundary of  $P$  into consecutive vertices that share the same farthest neighbor and edges of  $P$  whose endpoints have distinct farthest neighbors.

Using a result from Hersherberger and Suri [13], in  $O(n)$  time we can compute the farthest neighbor of each vertex of  $P$ . Recall that the farthest neighbor of each vertex of  $P$  is always a convex vertex of  $P$  [3] and is unique by our general position assumption.

We mark the vertices of  $P$  that are farthest neighbors of at least one vertex of  $P$ . Let  $M$  denote the set of marked vertices of  $P$  (clearly this set can be computed in  $O(n)$  time after

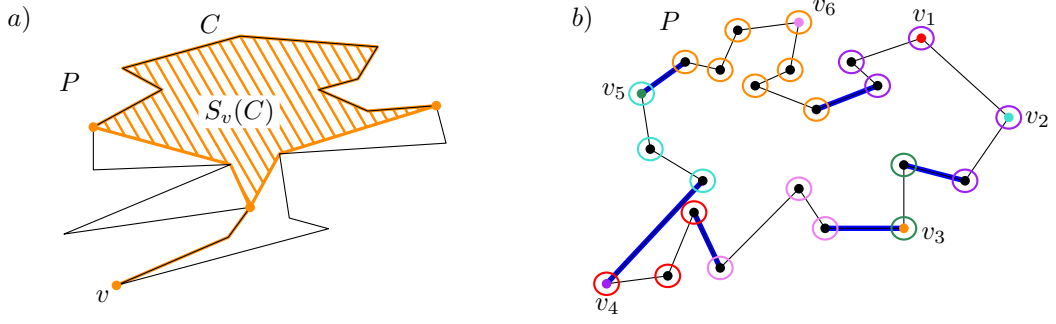


**Figure 2** a) The funnel  $S_v(C)$  of a vertex  $v$  and a chain  $C$  contained in  $\partial P$  are depicted. b) Each vertex of the boundary of  $P$  is assigned with a farthest neighbor which is then marked. The boundary is then decomposed into vertex disjoint chains, each associated with a marked vertex, joined by transition edges (blue) whose endpoints have different farthest neighbors.

193 applying the result of Hershberger and Suri). In other words,  $M$  contains all vertices of  $P$   
 194 whose Voronoi region contains at least one vertex of  $P$ .

195 Given a vertex  $v$  of  $P$ , the vertices of  $P$  whose farthest neighbor is  $v$  appear contiguously  
 196 along  $\partial P$  [2]. Therefore, after computing all these farthest neighbors, we effectively split the  
 197 boundary into subchains, each associated with a different vertex of  $M$ ; see Figure 2 (b).

198 Let  $a$  and  $b$  be the endpoints of a transition edge of  $\partial P$  such that  $a$  appears before  $b$  in  
 199 the clockwise order along  $\partial P$ . Because  $ab$  is a transition edge, we know that  $f(a) \neq f(b)$ .  
 200 Recall that we have computed  $f(a)$  and  $f(b)$  in the previous step and note that  $f(a)$  appears  
 201 also before  $f(b)$  along this clockwise order. For every vertex  $v$  that lies between  $f(a)$  and  $f(b)$   
 202 in the bottom chain of  $H_{ab}$ , we know that there cannot be a vertex  $u$  of  $P$  such that  $f(u) = v$ .  
 203 As proved by Aronov et al. [2, Corollary 2.7.4], if there is a point  $x$  on  $\partial P$  whose farthest  
 204 neighbor is  $v$ , then  $x$  must lie on the open segment  $(a, b)$ . In other words, the Voronoi region  
 205  $R(v)$  restricted to  $\partial P$  is contained in  $(a, b)$ .

## 206 4 Building hourglasses

207 Let  $E$  be the set of transition edges of  $\partial P$ . Given a transition edge  $ab \in E$ , we say that  $H_{ab}$  is a  
 208 *transition hourglass*. In order to construct the triangle cover of  $P$ , we construct the transition  
 209 hourglass of each transition edge of  $E$ . By Lemma 6, we know that  $\sum_{ab \in E} |H_{ab}| = O(n)$ .  
 210 Therefore, our aim is to compute the cover in time proportional to the size of  $H_{ab}$ .

211 By Lemma 3 we can compute a set of  $O(1)$  separating paths such that for each transition  
 212 edge  $ab$ , the transition hourglass  $H_{ab}$  is separated by one (or more) paths in this set. For each  
 213 endpoint of the  $O(1)$  separating paths we compute its shortest-path tree [10]. In addition,  
 214 we preprocess these trees in linear time to support LCA queries [12]. Both computations  
 215 need linear time per endpoint and use  $O(n)$  space. Since we do this process for a constant  
 216 number of endpoints, overall this preprocessing takes  $O(n)$  time.

217 Let  $\gamma$  be a separating path whose endpoints are  $x$  and  $y$ . Note that  $\gamma$  separates the  
 218 boundary of  $P$  into two chains  $S$  and  $S'$  such that  $S \cup S' = \partial P$ . Let  $\mathcal{H}(\gamma)$  be the set of each  
 219 transition hourglass separated by  $\gamma$  whose transition edge is contained in  $S$  (whenever an  
 220 hourglass is separated by more than one path, we pick one arbitrarily). Note that we can  
 221 classify all transition hourglasses into the sets  $\mathcal{H}(\gamma)$  in  $O(n)$  time (since  $O(1)$  separating  
 222 paths are considered).

223 We claim that we can compute all transition hourglass of  $\mathcal{H}(\gamma)$  in  $O(n)$  time. By

construction, the wall of each of these hourglasses consists of a (geodesic) path that connects a point in  $S$  with a point in  $S'$ . Let  $u \in S$  and  $v \in S'$  be two vertices such that  $\pi(u, v)$  is the wall of a hourglass in  $\mathcal{H}(\gamma)$ . Because LCA queries can be answered in  $O(1)$  time [12], Lemma 5 allows us to compute this path in  $O(|\pi(u, v)|)$  time. Therefore, we can compute all hourglasses of  $\mathcal{H}(\gamma)$  in  $O(\sum_{H \in \mathcal{H}(\gamma)} |H| + n) = O(n)$  time by Lemma 6. Because only  $O(1)$  separating paths are considered, we obtain the following result.

► **Lemma 8.** *We can construct the transition hourglass of all transition edges of  $P$  in  $O(n)$  time.*

## 5 Covering the polygon with apexed triangles

An *apexed triangle*  $\Delta = (a, b, c)$  with *apex*  $a$  is a triangle contained in  $P$  with an associated distance function  $g_\Delta(x)$ , called the *apex function* of  $\Delta$ , such that (1)  $a$  is a vertex of  $P$ , (2)  $b, c \in \partial P$ , and (3) there is a vertex  $w$  of  $P$ , called the *definer* of  $\Delta$ , such that

$$g_\Delta(x) = \begin{cases} -\infty & \text{if } x \notin \Delta \\ |xa| + |\pi(a, w)| = |\pi(x, w)| & \text{if } x \in \Delta \end{cases}$$

In this section, we show how to find a set of  $O(n)$  apexed triangles of  $P$  such that the upper envelope of their apex functions coincides with  $F_P(x)$ . To this end, we first decompose the transition hourglasses into apexed triangles that encode all the geodesic distance information inside them. For each marked vertex  $v \in M$  we construct a funnel that contains the Voronoi region of  $v$ . We then decompose this funnel into apexed triangles that encode the distance from  $v$ .

### 5.1 Inside the transition hourglass

Let  $ab$  be a transition edge of  $P$  such that  $b$  is the clockwise neighbor of  $a$  along  $\partial P$ . Let  $B_{ab}$  denote the bottom chain of  $H_{ab}$  after removing its endpoints. As noticed above, a point on  $\partial P$  can be farthest from a vertex in  $B_{ab}$  only if it lies in the open segment  $ab$ . That is, if  $v$  is a vertex of  $B_{ab}$  such that  $R(v) \neq \emptyset$ , then  $R(v) \cap \partial P \subset ab$ .

In fact, not only this Voronoi region is inside  $H_{ab}$  when restricted to the boundary of  $P$ , but also  $R(v) \subset H_{ab}$ . The next result follows trivially from Lemma 7.

► **Corollary 9.** *Let  $v$  be a vertex of  $B_{ab}$ . If  $R(v) \neq \emptyset$ , then  $R(v) \subset H_{ab}$ .*

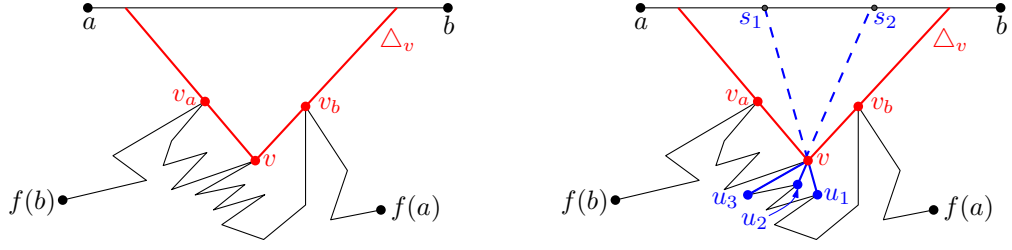
Our objective is to compute  $O(|H_{ab}|)$  apexed triangles that cover  $H_{ab}$ , each with its distance function, such that the upper envelope of these apex functions coincides with  $F_P(x)$  restricted to  $H_{ab}$  where it “matters”.

The same approach was already used by Pollack et al. in [22, Section 3]. Given a segment contained in the interior of  $P$ , they show how to compute a linear number of apexed triangles such that  $F_P(x)$  coincides with the upper envelope of the corresponding apex functions in the given segment.

While the construction we follow is analogous, we use it in the transition hourglass  $H_{ab}$  instead of the full polygon  $P$ . Therefore, we have to specify what is the relation between the upper envelope of the computed functions and  $F_P(x)$ . We will show that the upper envelope of the apex functions computed in  $H_{ab}$  coincides with  $F_P(x)$  inside the Voronoi region  $R(v)$  of every vertex  $v \in B_{ab}$ .

Let  $T_a$  and  $T_b$  be the shortest-path trees in  $H_{ab}$  from  $a$  and  $b$ , respectively. Assume that  $T_a$  and  $T_b$  are rooted at  $a$  and  $b$ , respectively. We can compute these trees in  $O(|H_{ab}|)$





■ **Figure 3** (left) A vertex  $v$  visible from the segment  $ab$  lying on the bottom chain of  $H_{ab}$ , and the triangle  $\Delta_v$  which contains the portion of  $ab$  visible from  $v$ . (right) The children  $u_1$  and  $u_2$  of  $v$  are visible from  $ab$  while  $u_3$  is not. The triangle  $\Delta_v$  is split into apexed triangles by the rays going from  $u_1$  and  $u_2$  to  $v$ .

time [10]. For each vertex  $v$  between  $f(a)$  and  $f(b)$ , let  $v_a$  and  $v_b$  be the neighbors of  $v$  in the paths  $\pi(v, a)$  and  $\pi(v, b)$ , respectively. We say that a vertex  $v$  is *visible* from  $ab$  if  $v_a \neq v_b$ . Note that if a vertex is visible, then the extension of these segments must intersect the top segment  $ab$ . Therefore, for each visible vertex  $v$ , we obtain a triangle  $\Delta_v$  as shown in Figure 3.

We further split  $\Delta_v$  into a series of triangles with apex at  $v$  as follows: Let  $u$  be a child of  $v$  in either  $T_a$  or  $T_b$ . As noted by Pollack et al.,  $v$  can be of three types, either (1)  $u$  is not visible from  $ab$  (and is hence a child of  $v$  in both  $T_a$  and  $T_b$ ); or (2)  $u$  is visible from  $ab$ , is a child of  $v$  only in  $T_b$ , and  $v_bvu$  is a left turn; or (3)  $u$  is visible from  $ab$ , is a child of  $v$  only in  $T_a$ , and  $v_avu$  is a right turn.

Let  $u_1, \dots, u_{k-1}$  be the children of  $v$  of type (2) sorted in clockwise order around  $v$ . Let  $c(v)$  be the maximum distance from  $v$  to any invisible vertex in the subtrees of  $T_a$  and  $T_b$  rooted at  $v$ ; if no such vertex exists, then  $c(v) = 0$ . Define a function  $d_l(v)$  on each vertex  $v$  of  $H_{ab}$  in a recursive fashion as follows: If  $v$  is invisible from  $ab$ , then  $d_l(v) = c(v)$ . Otherwise, let  $d_l(v)$  be the maximum of  $c(v)$  and  $\max\{d_l(u_i) + |u_iv| : u_i \text{ is a child of } v \text{ of type (2)}\}$ . Similarly we define a symmetric function  $d_r(v)$  using the children of type (3) of  $v$ .

For each  $1 \leq i \leq k-1$ , extend the segment  $u_iv$  past  $v$  until it intersects  $ab$  at a point  $s_i$ . Let  $s_0$  and  $s_k$  be the intersections of the extensions of  $vv_a$  and  $vv_b$  with the segment  $ab$ . We define then  $k$  triangles contained in  $\Delta_v$  as follows. For each  $0 \leq i \leq k-1$ , consider the triangle  $\Delta(s_i, v, s_{i+1})$  whose associated apexed (left) function is

$$f_i(x) = |xv| + \max_{j>i} \{c(v), |vu_j| + d_l(u_j)\}.$$

In a symmetric manner, we define a set of apexed triangles induced by the type (3) children of  $v$  and their respective apexed (right) functions.

Let  $g_1, \dots, g_r$  and  $\Delta_1, \dots, \Delta_r$  respectively be an enumeration of all the generated apex functions and triangles such that  $g_i$  is defined in the triangle  $\Delta_i$ . Because each function is determined uniquely by a pair of adjacent vertices in  $T_a$  or in  $T_b$ , and since these trees have  $O(|H_{ab}|)$  vertices, we conclude that  $r = O(|H_{ab}|)$ .

Note that for each  $1 \leq i \leq r$ , the triangle  $\Delta_i$  has two vertices on the segment  $ab$  and a third vertex, say  $a_i$ , called its *apex* such that for each  $x \in \Delta_i$ ,  $g_i(x) = |\pi(x, w_i)|$  for some vertex  $w_i$  of  $H_{ab}$ . We refer to  $w_i$  as the *definer* of  $\Delta_i$ . Intuitively,  $\Delta_i$  defines a portion of the geodesic distance function from  $w_i$  in a constant complexity region.

► **Lemma 10.** *Given a transition edge  $ab$  of  $P$ , we can compute a set  $\mathcal{A}_{ab}$  of  $O(|H_{ab}|)$  apexed triangles in  $O(|H_{ab}|)$  time with the property that for any point  $p \in P$  such that  $f(p) \in B_{ab}$ ,*



289 there is an apexed triangle  $\triangle \in \mathcal{A}_{ab}$  with apex function  $g$  and definer equal to  $f(p)$  such that  
 290 (1)  $p \in \triangle$  and (2)  $g(p) = F_P(p)$ .

291 In other words, Lemma 10 says that no information on farthest neighbors is lost if we  
 292 only consider the functions in  $\mathcal{A}_{ab}$  within  $H_{ab}$ . In the next section we use a similar approach  
 293 to construct a set of apexed triangles (and their corresponding apex functions), so as to  
 294 encode the distance from the vertices of  $M$ .

## 295 5.2 Inside the funnels of marked vertices

296 Recall that for each marked vertex  $v \in M$ , we know at least of one vertex on  $\partial P$  such that  $v$   
 297 is its farthest neighbor. For any marked vertex  $v$ , let  $u_1, \dots, u_{k-1}$  be the vertices of  $P$  such  
 298 that  $v = f(u_i)$  and assume that they appear in this order when traversing  $\partial P$  clockwise. Let  
 299  $u_0$  and  $u_k$  be the neighbors of  $u_1$  and  $u_{k-1}$  other than  $u_2$  and  $u_{k-2}$ , respectively. Note that  
 300 both  $u_0u_1$  and  $u_{k-1}u_k$  are transition edges of  $P$ . Thus, we can assume that their transition  
 301 hourglasses have been computed.

302 Let  $C_v = (u_0, \dots, u_k)$  and consider the funnel  $S_v(C_v)$ . We call  $C_v$  the *main chain*  
 303 of  $S_v(C_v)$  while  $\pi(u_k, v)$  and  $\pi(v, u_0)$  are referred to as the *walls* of the funnel. Because  
 304  $v = f(u_1) = f(u_{k-1})$ , we know that  $v$  is a vertex of both  $H_{u_0u_1}$  and  $H_{u_{k-1}u_k}$ . By definition,  
 305 we have  $\pi(v, u_0) \subset H_{u_0u_1}$  and  $\pi(v, u_k) \subset H_{u_{k-1}u_k}$ . Thus, we can explicitly compute both  
 306 paths  $\pi(v, u_0)$  and  $\pi(v, u_k)$  in  $O(|H_{u_0u_1}| + |H_{u_{k-1}u_k}|)$  time. So, overall, the funnel  $S_v(C_v)$   
 307 can be constructed in  $O(k + |H_{u_0u_1}| + |H_{u_{k-1}u_k}|)$  time. Recall that, by Lemma 6, the total  
 308 sum of the complexities of the transition hourglasses is  $O(n)$ . In particular, we can bound  
 309 the total time needed to construct the funnels of all marked vertices by  $O(n)$ .

Since the complexity of the walls of these funnels is bounded by the complexity of the  
 transition hourglasses used to compute them, we get that

$$\sum_{v \in M} |S_v(C_v)| = O\left(n + \sum_{ab \in E} |H_{ab}|\right) = O(n).$$

310 ► **Lemma 11.** *Let  $x$  be a point in  $P$ . If  $v = f(x)$  is a vertex of  $M$ , then  $x \in S_v(C_v)$ .*

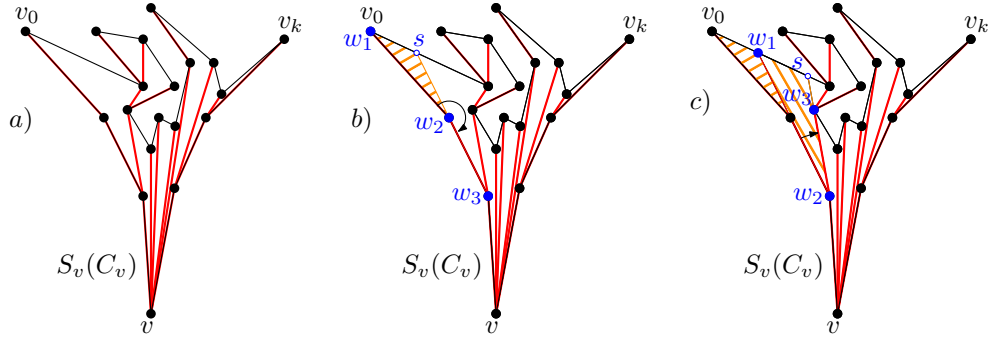
311 We now proceed to split a given funnel into  $O(|S_v(C_v)|)$  apexed triangles that encode the  
 312 distance function from  $v$ . To this end, we compute the shortest-path tree  $T_v$  of  $v$  in  $S_v(C_v)$   
 313 in  $O(|S_v(C_v)|)$  time [11]. We consider the tree  $T_v$  to be rooted at  $v$  and assume that for each  
 314 node  $u$  of this tree we have stored the geodesic distance  $|\pi(u, v)|$ .

315 Start an Eulerian tour from  $v$  walking in a clockwise order of the edges. Let  $w_1$  be  
 316 the first leaf of  $T_v$  found, and let  $w_2$  and  $w_3$  be the next two vertices visited in the traversal.  
 317 Two cases arise:

318 **Case 1:**  $w_1, w_2, w_3$  makes a right turn. We define  $s$  as the first point hit by the ray  
 319 apexed at  $w_2$  that shoots in the direction opposite to  $w_3$ .

320 We claim that  $w_1$  and  $s$  lie on the same edge of the boundary of  $S_v(C_v)$ . Otherwise,  
 321 there would be a vertex  $u$  visible from  $w_2$  inside the wedge with apex  $w_2$  spanned by  $w_1$  and  
 322  $w_3$ . Note that the first edge of the path  $\pi(u, v)$  is the edge  $uw_2$ . Therefore,  $uw_2$  belongs to  
 323 the shortest-path  $T_v$  contradicting the Eulerian order in which the vertices of this tree are  
 324 visited as  $u$  should be visited before  $w_3$ . Thus,  $s$  and  $w_1$  lie on the same edge and  $s$  can be  
 325 computed in  $O(1)$  time.

326 At this point, we construct the apexed triangle  $\triangle(w_2, w_1, s)$  apexed at  $w_2$  with apex  
 327 function  $g(x) = |xw_2| + |\pi(w_2, v)|$ . We modify tree  $T_v$  by removing the edge  $w_1w_2$  and  
 328 replacing the edge  $w_3w_2$  by the edge  $w_3s$ ; see Figure 4.



■ **Figure 4** The funnel  $S_v(C_v)$  and the shortest-path tree from  $v$  are depicted in (a). The two cases of the algorithm described in Lemma 12 are shown in (b) and (c).

329 **Case 2:**  $w_1, w_2, w_3$  makes a left turn and  $w_1$  and  $w_3$  are adjacent, then if  $w_1$  and  $w_3$  lie  
 330 on the same edge of  $\partial P$ , we construct an apexed triangle  $\triangle(w_2, w_1, w_3)$  apexed at  $w_2$  with  
 331 apex function  $g(x) = |xw_2| + |\pi(w_2, v)|$ . Otherwise, let  $s$  be the first point of the boundary  
 332 of  $S_v(C_v)$  hit by the ray shooting from  $w_3$  in the direction opposite to  $w_2$ .

333 By the same argument as above, we can show that  $w_1$  and  $s$  lie on the same edge of  
 334 the boundary of  $S_v(C_v)$  (and thus, we can compute  $s$  in  $O(1)$  time). We construct an  
 335 apexed triangle  $\triangle(w_2, w_1, s)$  apexed at  $w_2$  with apex function  $g(x) = |xw_2| + |\pi(w_2, v)|$ . We  
 336 modify the tree  $T_v$  by removing the edge  $w_1w_2$  and adding the edge  $w_3s$ ; see Figure 4 for an  
 337 illustration.

338 ► **Lemma 12.** *The above procedure runs in  $O(|S_v(C_v)|)$  time and computes  $O(|S_v(C_v)|)$   
 339 interior disjoint apexed triangles such that their union covers  $S_v(C_v)$ . Moreover, for each  
 340 point  $x \in R(v)$ , there is an apexed triangle  $\triangle$  with apex function  $g(x)$  such that (1)  $x \in \triangle$   
 341 and (2)  $g(x) = F_P(x)$ .*

## 342 6 Prune and search

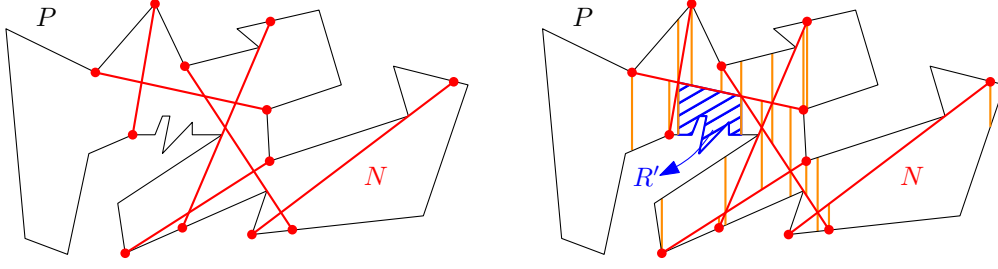
343 With the tools introduced in the previous sections, we can proceed to give the prune and  
 344 search algorithm to compute the geodesic center. The idea of the algorithm is to partition  $P$   
 345 into  $O(1)$  cells, determine on which cell of  $P$  the center lies and recurse on that cell as a new  
 346 subproblem with smaller complexity.

347 Naturally, we can discard all apexed triangles that do not intersect the new cell containing  
 348 the center. Using the properties of the cutting, we can show that both the complexity of the  
 349 cell containing the center, and the number of apexed triangles that intersect it decrease by  
 350 a constant fraction in each iteration of the algorithm. This process is then repeated until  
 351 either of the two objects has constant descriptive size.

352 Let  $\tau$  be the set all apexed triangles computed in previous sections. Lemmas 6 and 12  
 353 directly provide a bound on the complexity of  $\tau$ .

354 ► **Corollary 13.** *The set  $\tau$  consists of  $O(n)$  apexed triangles.*

355 Let  $\phi(x)$  be the upper envelope of the apex functions of every triangle in  $\tau$  (i.e.,  $\phi(x) =$   
 356  $\max\{g_i(x) : g_i(x) \in \tau, x \in \triangle_i\}$ ). The following result is a direct consequence of Lemmas 10  
 357 and 12, and shows that the  $O(n)$  apexed triangles of  $\tau$  not only cover  $P$ , but their apex  
 358 functions suffice to reconstruct the function  $F_P(x)$ .



■ **Figure 5** The  $\epsilon$ -net  $N$  splits  $P$  into  $O(1)$  sub-polygons that are further refined into a 4-cell decomposition using  $O(1)$  ray-shooting queries from the vertices of the arrangement defined by  $N$ .

359 ► **Lemma 14.** *The functions  $\phi(x)$  and  $F_P(x)$  coincide in the domain of points of  $P$ , i.e., for*  
 360 *each  $p \in P$ ,  $\phi(p) = F_P(p)$ .*

361 Given a chord  $C$  of  $P$  a *half-polygon* of  $P$  is one of the two simple polygons in which  
 362  $C$  splits  $P$ . A *4-cell* of  $P$  is a simple polygon obtained as the intersection of at most four  
 363 half-polygons. Because a 4-cell is the intersection of geodesically convex sets, it is also  
 364 geodesically convex.

365 Let  $R$  be a 4-cell of  $P$  and let  $\tau_R$  be the set of apexed triangles of  $\tau$  that intersect  $R$ .  
 366 Let  $m_R = \max\{|R|, |\tau_R|\}$ . Recall that, by construction of the apexed triangles, for each  
 367 triangle of  $\tau_R$  at least one and at most two of its boundary segments is a chord of  $P$ . Let  $\mathcal{C}$   
 368 be the set containing all chords that belong to the boundary of a triangle of  $\tau_R$ . Therefore,  
 369  $|\tau_R| \leq |\mathcal{C}| \leq 2|\tau_R|$ .

370 To construct an  $\epsilon$ -net of  $\mathcal{C}$ , we need some definitions (for more information on  $\epsilon$ -nets refer  
 371 to [17]). Let  $\varphi$  be the set of all open 4-cells of  $P$ . For each  $t \in \varphi$ , let  $\mathcal{C}_t = \{C \in \mathcal{C} : C \cap t \neq \emptyset\}$   
 372 be the set of chords of  $\mathcal{C}$  induced by  $t$ . Finally, let  $\varphi_{\mathcal{C}} = \{\mathcal{C}_t : t \in \varphi\}$  be the family of subsets  
 373 of  $\mathcal{C}$  induced by  $\varphi$ .

374 Let  $\epsilon > 0$  (the exact value of  $\epsilon$  will be specified later). Consider the range space  $(\mathcal{C}, \varphi_{\mathcal{C}})$   
 375 defined by  $\mathcal{C}$  and  $\varphi_{\mathcal{C}}$ . Because the VC-dimension of this range space is finite, we can compute  
 376 an  $\epsilon$ -net  $N$  of  $(\mathcal{C}, \varphi_{\mathcal{C}})$  in  $O(n/\epsilon) = O(n)$  time [17]. The size of  $N$  is  $O(\frac{1}{\epsilon} \log \frac{1}{\epsilon}) = O(1)$  and  
 377 its main property is that any 4-cell that does not intersect a chord of  $N$  will intersect at  
 378 most  $\epsilon|\mathcal{C}|$  chords of  $\mathcal{C}$ .

379 Observe that  $N$  partitions  $R$  into  $O(1)$  sub-polygons (not necessarily 4-cells). We further  
 380 refine this partition by performing a 4-cell decomposition. That is, we shoot vertical rays up  
 381 and down from each endpoint of  $N$ , and from the intersection point of any two segments  
 382 of  $N$ , see Figure 5. Overall, this partitions  $R$  into  $O(1)$  4-cells such that each either (i) is  
 383 a convex polygon contained in  $P$  of at most four vertices, or otherwise (ii) contains some  
 384 chain of  $\partial P$ . Since  $|N| = O(1)$ , the whole decomposition can be computed in  $O(m_R)$  time  
 385 (the intersections between segments of  $N$  are done in constant time, and for the ray shooting  
 386 operations we walk along the boundary of  $R$  once).

387 In order to determine which 4-cell contains the geodesic center of  $P$ , we extend each edge  
 388 of a 4-cell to a chord  $C$ . This can be done with two ray-shooting queries (each of which  
 389 takes  $O(m_R)$  time). We then use the chord-oracle from Pollack et al. [22, Section 3] to decide  
 390 which side of  $C$  contains  $c_P$ . The only requirement of this technique is that the function  
 391  $F_P(x)$  coincides with the upper envelope of the apex functions when restricted to  $C$ . Which  
 392 is true by Lemma 14 and from the fact that  $\tau_R$  consists of all the apexed triangles of  $\tau$  that  
 393 intersect  $R$ .

394 Because the chord-oracle described by Pollack et al. [22, Section 3] runs in linear time on

the number of functions defined on  $C$ , we can decide in total  $O(m_R)$  time on which side of  $C$  the geodesic center of  $P$  lies. Since our decomposition into 4-cells has constant complexity, we need to perform  $O(1)$  calls to the oracle before determining the 4-cell  $R'$  that contains the geodesic center of  $P$ .

The chord-oracle computes the minimum of  $F_P(x)$  restricted to the chord before determining the side containing the minimum. In particular, if  $c_P$  lies on any chord bounding  $R'$ , then the chord-oracle will find it. Therefore, we can assume that  $c_P$  lies in the interior of  $R'$ . Moreover, since  $N$  is a  $\varepsilon$ -net, we know that at most  $\varepsilon|C|$  chords of  $C$  will intersect  $R'$ .

Using a similar argument, we can show that the complexity of  $R'$  also decreases: since  $|C| \leq 2|\tau_R| \leq 2m_R$ , we guarantee that at most  $2\varepsilon m_R$  apexed triangles intersect  $R'$ . Moreover, each vertex of  $R'$  is in at least one apexed triangle of  $\tau_R$  by Lemma 14, and by construction, each apexed triangle can cover at most three vertices. By the pigeonhole principle we conclude that  $R'$  can have at most  $6\varepsilon m_R$  vertices. Thus, if we choose  $\varepsilon = 1/12$ , we guarantee that both the size of the 4-cell  $R'$  and the number of apexed triangles in  $\tau_{R'}$  are at most  $m_R/2$ .

In order to proceed with the algorithm on  $R'$  recursively, we need to compute the set  $\tau_{R'}$  with the at most  $\varepsilon|C|$  apexed triangles of  $\tau_R$  that intersect  $R'$  (i.e., prune the apexed triangles that do not intersect with  $R'$ ). For each apexed triangle  $\triangle \in \tau_R$ , we can determine in constant time if it intersects  $R'$  (either one of the endpoints is in  $R' \cap \partial P$  or the two boundaries have non-empty intersection in the interior of  $P$ ). Overall, we need  $O(m_R)$  time to compute the at most  $\varepsilon|C|$  triangles of  $\tau_R$  that intersect  $R'$ .

By recursing on  $R'$ , we guarantee that after  $O(\log m_R)$  iterations, we reduce the size of either  $\tau_R$  or  $R'$  to constant. In the former case, the minimum of  $F_P(x)$  can be found by explicitly constructing function  $\phi$  in  $O(1)$  time. In the latter case, we triangulate  $R'$  and apply the chord-oracle to determine which triangle will contain  $c_P$ . The details needed to find the minimum of  $\phi(x)$  inside this triangle are giving the next section.

► **Lemma 15.** *In  $O(n)$  time we can find either the geodesic center of  $P$  or a triangle containing the geodesic center.*

## 7 Solving the problem restricted to a triangle

In order to complete the algorithm it remains to show how to find the geodesic center of  $P$  for the case in which  $R'$  is a triangle. If this triangle is in the interior of  $P$ , it may happen that several apexed triangles of  $\tau$  fully contain  $R'$ . Thus, the pruning technique used in the previous section cannot be further applied. We solve this case with a different approach.

Recall that  $\phi(x)$  denotes the upper envelope of the apex functions of the triangles in  $\tau$ , and the geodesic center is the point that minimizes  $\phi$ . The key observation is that, as it happened with chords, the function  $\phi(x)$  restricted to  $R'$  is convex.

Let  $\triangle_1, \triangle_2, \dots, \triangle_m$  be the set of  $m = O(n)$  apexed triangles of  $\tau$  that intersect  $R'$ . Let  $g_i(x) = |xa_i| + \kappa_i$  be the apex function of  $\triangle_i$ , where  $a_i$  and  $w_i$  are the apex and the definer of  $\triangle_i$ , respectively, and  $\kappa_i = |\pi(a_i, w_i)|$  is a constant.

By Lemma 14,  $\phi(x) = F_P(x)$ . Therefore, the problem of finding the center is equivalent to the following optimization problem in  $\mathbb{R}^3$ :

(P1). Find a point  $(x, r) \in \mathbb{R}^3$  minimizing  $r$  subject to  $x \in R'$  and

$$g_i(x) = |xa_i| + \kappa_i \leq r, \text{ if } x \in \triangle_i \text{ for } 1 \leq i \leq m.$$

Thus, we need only to find the solution to (P1) to find the geodesic center of  $P$ . A similar optimization was studied by Megiddo in [18]. The main difference being that we have apex functions, defined only in their corresponding apexed triangles, instead of functions defined

in the entire plane. We use some remarks described by Megiddo in order to simplify the description of (P1). To simplify the formulas, we square the equations:

$$\|x\|^2 - 2x \cdot a_i + \|a_i\|^2 = |xa_i|^2 \leq (r - \kappa_i)^2 = r^2 - 2r\kappa_i + \kappa_i^2.$$

And finally for each  $1 \leq i \leq m$ , we define the function  $h_i(x, r)$  as follows:

$$h_i(x, r) = \|x\|^2 - 2x \cdot a_i + \|a_i\|^2 - r^2 + 2r\kappa_i - \kappa_i^2 \leq 0$$

Therefore, our optimization problem can be reformulated as:

**(P2).** Find a point  $(x, r) \in \mathbb{R}^3$  such that  $r$  is minimized subject to  $x \in R'$  and

$$h_i(x, r) \leq 0, \text{ if } x \in \triangle_i \text{ for } 1 \leq i \leq m.$$

. Although the functions  $h_i(x, r)$  are not linear, they all have the same non-linear terms. Therefore, for  $i \neq j$ , we get that  $h_i(x, r) = h_j(x, r)$  defines a *separating plane*

$$\gamma_{i,j} = \{(x, r) \in \mathbb{R}^3 : 2(\kappa_i - \kappa_j)r - 2(a_i - a_j) \cdot x + \|a_i\|^2 - \|a_j\|^2 - \kappa_i^2 + \kappa_j^2 = 0\}$$

As noted by Megiddo, this separating plane has the following property: If the solution  $(x, r)$  to our optimization problem is known to lie to one side of  $\gamma_{i,j}$ , then we know that one of the constraints is redundant.

In Megiddo's problem, it sufficed to have a *side-decision oracle* to determine on which side of a plane  $\gamma_{i,j}$  the solution lies. Megiddo showed how to implement this oracle in a way that the running time is proportional to the number of constraints [18].

Once we have such an oracle, we can proceed with the prune and search similar to the one introduced in Section 6: pair the functions arbitrarily, and consider the set of  $m/2$  separating planes defined by these pairs. For some constant  $r$ , compute a  $1/r$ -cutting in  $\mathbb{R}^3$  of the separating planes. An  $1/r$ -cutting is a partition of the plane into  $O(r^2)$  convex regions each of which is of constant size and intersects at most  $m/2r$  separating planes. A cutting of planes can be computed in linear time in  $\mathbb{R}^3$  for any  $r = O(1)$  [16]. After computing the cutting, determine in which of the regions the minimum lies by performing  $O(1)$  calls to the side-decision oracle. Because at least  $(r - 1)m/2r$  separating planes do not intersect this constant size region, for each of them we can discard one of the constraints as it becomes redundant. Repeating this algorithm recursively we obtain a linear running time.

In this paper, we follow a similar approach, but our set of separating planes needs to be extended in order to handle apex functions as they are only defined in a triangular domain. Note that the vertices of each apexed triangle that intersect  $R'$  have their endpoints either outside of  $R'$  or on its boundary.

## 7.1 Optimization problem in a convex domain

In this section we describe our algorithm to solve the optimization problem (P2). To this end, we pair the apexed triangles arbitrarily to obtain  $m/2$  pairs. By identifying the plane where  $P$  lies with the plane  $Z_0 = \{(x, y, z) : z = 0\}$ , we can embed each apexed triangle in  $\mathbb{R}^3$ . A *plane-set* is a set consisting of at most five planes in  $\mathbb{R}^3$ . For each pair of apexed triangles  $(\triangle_i, \triangle_j)$  we define a plane-set as follows: For each chord bounding either  $\triangle_i$  or  $\triangle_j$ , consider the line extending this chord and the vertical extrusion of this line in  $\mathbb{R}^3$ , i.e., the plane containing this chord orthogonal to  $Z_0$ . Moreover, consider the separating plane  $\gamma_{i,j}$ . The set containing these planes is the plane-set of the pair  $(\triangle_i, \triangle_j)$ .

Let  $\Gamma$  be the union of all the plane-sets defined by the  $m/2$  pairs of apexed triangles. Thus,  $\Gamma$  is a set that consists of  $O(m)$  planes. Compute a  $1/r$ -cutting of  $\Gamma$  in  $O(m)$  time for

some constant  $r$  to be specified later. Because  $r$  is constant, this  $1/r$ -cutting splits the space into  $O(1)$  convex regions, each bounded by a constant number of planes [16]. By using a side-decision algorithm (to be specified later), we can determine the region  $Q$  of the cutting that contains the solution to (P2). Because  $Q$  is the region of a  $1/r$ -cutting of  $\Gamma$ , we know that at most  $|\Gamma|/r$  planes of  $\Gamma$  intersect  $Q$ . In particular, at most  $|\Gamma|/r$  plane-sets intersect  $Q$  and hence, at least  $(r-1)|\Gamma|/r$  plane-sets do not intersect  $Q$ .

Let  $(\Delta_i, \Delta_j)$  be a pair such that its plane-set does not intersect  $Q$ . Let  $Q'$  be the projection of  $Q$  on the plane  $Z_0$ . Because the plane-set of this pair does not intersect  $Q$ , we know that  $Q'$  intersects neither the boundary of  $\Delta_i$  nor that of  $\Delta_j$ . Two cases arise:

**Case 1.** If either  $\Delta_i$  or  $\Delta_j$  does not intersect  $Q'$ , then we know that their apex function is redundant and we can drop the constraint associated with this apexed triangle.

**Case 2.** If  $Q' \subset \Delta_i \cap \Delta_j$ , then we need to decide which constraint to drop. To this end, we consider the separating plane  $\gamma_{i,j}$ . Notice that inside the vertical extrusion of  $\Delta_i \cap \Delta_j$  (and hence in  $Q$ ), the plane  $\gamma_{i,j}$  has the property that if we know its side containing the solution, then one of the constraints can be dropped. Since  $\gamma_{i,j}$  does not intersect  $Q$  as  $\gamma_{i,j}$  belongs to the plane-set of  $(\Delta_i, \Delta_j)$ , we can decide which side of  $\gamma_{i,j}$  contains the solution to (P2) and drop one of the constraints.

Regardless of the case if the plane-set of a pair  $(\Delta_i, \Delta_j)$  does not intersect  $Q$ , then we can drop one of its constraints. Since at least  $(r-1)|\Gamma|/r$  plane-sets do not intersect  $Q$ , we can drop at least  $(r-1)|\Gamma|/r$  constraints. Because  $|\Gamma| \geq m/2$  as each plane-set contains at least one plane, by choosing  $r = 2$ , we are able to drop at least  $|\Gamma|/2 \geq m/4$  constraints. Consequently, after  $O(m)$  time, we are able to drop  $m/4$  apexed triangles. By repeating this process recursively, we end up with a constant size problem in which we can compute the upper envelope of the functions explicitly and find the solution to (P2) using exhaustive search. Thus, the running time of this algorithm is bounded by the recurrence  $T(m) = T(3m/4) + O(m)$  which solves to  $O(m)$ . Because  $m = O(n)$ , we can find the solution to (P2) in  $O(n)$  time.

The last detail is the implementation of the side-decision algorithm. Given a plane  $\gamma$ , we want to decide on which side lies the solution to (P2). To this end, we solve (P2) restricted to  $\gamma$ , i.e., with the additional constraint of  $(x, r) \in \gamma$ . This approach was used by Megiddo [18], the idea is to recurse by reducing the dimension of the problem. Another approach is to use a slight modification of the chord-oracle described by Pollack et al. [22, Section 3].

Once the solution to (P2) restricted to  $\gamma$  is known, we can follow the same idea used by Megiddo [18] to find the side of  $\gamma$  containing the global solution to (P2). Intuitively, we find the apex functions that define the minimum restricted to  $\gamma$ . Since  $\phi(x) = F_P(x)$  is locally defined by these functions, we can decide on which side the minimum lies using convexity. We obtain the following result.

► **Lemma 16.** *Let  $R'$  be a convex trapezoid contained in  $P$  such that  $R'$  contains the geodesic center of  $P$ . Given the set of all apexed triangles of  $\tau$  that intersect  $R'$ , we can compute the geodesic center of  $P$  in  $O(n)$  time.*

The following theorem summarizes the results presented in this paper.

► **Theorem 17.** *We can compute the geodesic center of any simple polygon  $P$  of  $n$  vertices in  $O(n)$  time.*



## References

- 1 B. Aronov. On the geodesic Voronoi diagram of point sites in a simple polygon. *Algorithmica*, 4(1-4):109–140, 1989.
- 2 B. Aronov, S. Fortune, and G. Wilfong. The furthest-site geodesic Voronoi diagram. *Discrete & Computational Geometry*, 9(1):217–255, 1993.
- 3 T. Asano and G. Toussaint. Computing the geodesic center of a simple polygon. Technical Report SOCS-85.32, McGill University, 1985.
- 4 S. W. Bae, M. Korman, and Y. Okamoto. The geodesic diameter of polygonal domains. *Discrete & Computational Geometry*, 50(2):306–329, 2013.
- 5 S. W. Bae, M. Korman, and Y. Okamoto. Computing the geodesic centers of a polygonal domain. In *Proc. of CCCG*, 2014.
- 6 S. W. Bae, M. Korman, Y. Okamoto, and H. Wang. Computing the  $L_1$  geodesic diameter and center of a simple polygon in linear time. In *Proc. of LATIN*, pages 120–131, 2014.
- 7 B. Chazelle. A theorem on polygon cutting with applications. In *Proc. of FOCS*, pages 339–349, 1982.
- 8 H. Djidjev, A. Lingas, and J.-R. Sack. An  $O(n \log n)$  algorithm for computing the link center of a simple polygon. *Discrete & Computational Geometry*, 8:131–152, 1992.
- 9 H. Edelsbrunner and E. P. Mücke. Simulation of simplicity: a technique to cope with degenerate cases in geometric algorithms. *ACM Transactions on Graphics*, 9(1):66–104, 1990.
- 10 L. Guibas, J. Hershberger, D. Leven, M. Sharir, and R. E. Tarjan. Linear-time algorithms for visibility and shortest path problems inside triangulated simple polygons. *Algorithmica*, 2(1-4):209–233, 1987.
- 11 L. J. Guibas and J. Hershberger. Optimal shortest path queries in a simple polygon. In *Proc. of STOC*, pages 50–63, 1987.
- 12 D. Harel and R. E. Tarjan. Fast algorithms for finding nearest common ancestors. *SIAM Journal on Computing*, 13(2):338–355, 1984.
- 13 J. Hershberger and S. Suri. Matrix searching with the shortest path metric. In *Proc. of STOC*, pages 485–494, 1993.
- 14 Y. Ke. An efficient algorithm for link-distance problems. In *Proc. of SoCG*, pages 69–78, 1989.
- 15 D.-T. Lee and F. P. Preparata. Euclidean shortest paths in the presence of rectilinear barriers. *Networks*, 14(3):393–410, 1984.
- 16 J. Matoušek. Approximations and optimal geometric divide-and-conquer. In *Proc. of STOC*, pages 505–511, 1991.
- 17 J. Matoušek. Construction of epsilon nets. In *Proc. of SoCG*, pages 1–10, New York, 1989.
- 18 N. Megiddo. On the ball spanned by balls. *Discrete & Computational Geometry*, 4(1):605–610, 1989.
- 19 J. S. B. Mitchell. Geometric shortest paths and network optimization. In J.-R. Sack and J. Urrutia, editors, *Handbook of Computational Geometry*, pages 633–701. Elsevier, 2000.
- 20 B. Nilsson and S. Schuierer. Computing the rectilinear link diameter of a polygon. In *Proc. of CG*, pages 203–215, 1991.
- 21 B. Nilsson and S. Schuierer. An optimal algorithm for the rectilinear link center of a rectilinear polygon. *Computational Geometry: Theory and Applications*, 6:169–194, 1996.
- 22 R. Pollack, M. Sharir, and G. Rote. Computing the geodesic center of a simple polygon. *Discrete & Computational Geometry*, 4(1):611–626, 1989.
- 23 S. Suri. *Minimum Link Paths in Polygons and Related Problems*. PhD thesis, Johns Hopkins Univ., 1987.
- 24 S. Suri. Computing geodesic furthest neighbors in simple polygons. *Journal of Computer and System Sciences*, 39(2):220–235, 1989.